Desalination and Water Treatment
www.deswater.com
doi: 10.5004/dwt.2021.27708

237 (2021) 1–17
October

Experimental and numerical studies on predicting and improving the full-scale wastewater treatment plant hydrodynamics

Rahim Şibil[a,*], Egemen Aras[b], Murat Kankal[c]

[a]*Department of Civil Engineering, Faculty of Engineering and Natural Sciences, University of Gümüşhane, Gümüşhane 29100, Turkey, email: rahimsibil@gumushane.edu.tr*
[b]*Department of Civil Engineering, Faculty of Engineering and Natural Sciences, University of Bursa Technical, Bursa, Turkey, email: egemen.aras@btu.edu.tr*
[c]*Department of Civil Engineering, Faculty of Engineering, University of Bursa Uludağ, Bursa 16059, Turkey, email: mkankal@uludag.edu.tr*

Received 27 January 2021; Accepted 12 August 2021

ABSTRACT

This paper presents the results of both experimental and numerical studies on biological wastewater treatment plant (WWTP), oxidation ditches (OD) hydrodynamics to design and develop the desired flow conditions of the WWTP. Computational fluid dynamics (CFD) models were developed using CFD software, ANSYS Fluent (V13) with the three-dimensional, steady, incompressible flow based on the Reynolds-Averaged Navier-Stokes equations for flow field calculations in the combined ODs. Also, three different turbulence models [standard k–ε (ske), renormalization group k–ε (RNG), and realizable k–ε (real)] were performed for a comparative study. The numerical model was verified based on the experimental data in the relative errors for ske, RNG, and real 13%, 17%, and 18%, respectively. According to the parametric studies, the hydrodynamic characteristics of the existing WWTP were investigated. The maximum wastewater velocity occurred at the inlet and outlet, affecting the flow field in ODs. Moreover, the water velocity decreased as it moved away from the inlet and outlet locations at vertical and horizontal. It can also be noted that there was no homogeneous flow field distribution in ODs. Because the current OD model needs improvement hydrodynamically, a new original OD geometry was presented to eliminate the hydraulic weakness of existing WWTP by CFD analysis. The new original geometry provides a more homogeneous flow field in ODs that mean it will also help treatment efficiency and energy saving according to the operating principles of this facility.

Keywords: Computational fluid dynamics modeling; Oxidation ditch; Turbulence modeling; Acoustic Doppler Velocimeter

1. Introduction

Oxidation ditches (ODs) are a modified form of the activated sludge biological treatment method. Today, it has a wide usage area due to its advantages such as reliability, ease of operation, and low sludge production. The ideal flow model is plug-flow and no return. With its oval or channel structure equipped with mechanical aerators, the plug-flow provides a single tank with the benefits of flow and full-mix reactors. The hydrodynamic character and flow behavior take part in meaningful roles in the design and operation of ODs. Hydrodynamic behaviors of ODs can be determined by simulation. Computational fluid dynamics (CFD) has been extensively used to model the variable hydraulic and biological events that may arise within biological tanks. Latterly, a completely new point of view of this discipline of study is provided by modeling

* Corresponding author.

the wastewater treatment plants (WWTPs) hydrodynamics by employing CFD methods, which let resolution other physical phenomena like aeration or settling processes [1]. Moreover, the latest developments in multiphase flow study have grown in the utilization of CFD modeling in wastewater treatment, concentrating on the design of physical and biological treatment units. In addition to that, CFD becomes famous compared to traditional WWT modeling approaches that enable the high-precision analysis of engineering systems that are costly, difficult, and even dangerous to reproduce on a laboratory scale, pilot scale, or field conditions [2].

In the previous studies, CFD analyzes were performed to determine the hydrodynamic characteristic of existing ODs in general. Although some studies have been given various suggestions to improve hydrodynamic characteristics, these improvements have generally been tried to be achieved by optimization of structural elements such as mixers and aerators within the facility [3–15]. From that point forth, this study aims to present models with hydrodynamically good, new, and original geometric shapes for ODs. CFD modeling was implemented for ODs with several new geometries in this context, and the most appropriate one was given. In addition, this study is unique in modeling ODs using pipes for inlet and outlet in CFD analysis. In previous studies, inlet and outlet were ignored in CFD analyses because their effects on the flow field calculations within the ditch were minimal [16]. Therefore, this study has not been carried out before examining the effects of inlet and outlet velocities on the velocity distribution in the ditch due to the continuity equation. The CFD software ANSYS Fluent (V13), with high predictive and simulation power, was used for analyses. Because of the difficulties of the full-scale field measurement, such as time-consuming, costly, complexity and lack of technical and physical equipment, the obtained measurement data to validate the numerical models were laboratory scale [4,8,9,11,13–15,17]. However, there were also full-scale measurement studies to validate the models. But in most of these studies, the measurement points were less than 4 [5,8–10], only in 2 studies the measurement points were 10 and 12 [6,12]. This study verified the model by taking data from 14 different points and proven a more systematic measurement network compared with other studies.

This study focused on the hydrodynamic behavior of ODs without external momentum sources such as air diffusers and impellers that consume more energy in operation than other activated sludge processes; to that end, both experimental and numerical studies were carried out assessing the hydrodynamic characteristics of the full-scale WWTP. Hence, a hydraulically suitable original geometry has been proposed according to CFD analysis results. Another goal of this study is to compare the different turbulence models performing in CFD analyses of ODs. In addition to that, the inlet and outlet are considered in the simulation, and their effects on the flow field in ODs are investigated. Although extensive research was carried out on modeling ODs, there is a lack of study on modeling the inlet and outlet as a pipe flow. Moreover, measurements were taken from 14 different points in a full-scale facility to provide a more systematic measurement network.

2. Materials and methods

2.1. Full-scale OD description

In this paper, the full-scale ODs, the biological treatment unit of Gümüşhane WWTP, located in Gümüşhane province, Turkey, with a treatment capacity of 3,945 m^3/d was selected. This unit comprises two ditches, each with a length of 40 m, a width of 10 m, and a depth of 6 m (Fig. 1). The maximum water level and the radius of the guiding wall in the ODs were 5.25 and 2.35 m, respectively. There were two inlets and one outlet. The effluent of the two ditches combine in a small compartment and discharge together in a common outlet. The inner diameter of the inlet pipes is 35 cm, and the outlet pipe diameter is 50 cm with the 5 cm pipe wall thickness.

The wastewater characterization is crucial at all stages of plant design. For example, the five-day-biological oxygen demand (BOD_5) value which is the most used parameter of organic pollution and comprises the amount of the dissolved oxygen used by microorganisms in the biological oxidation of organic matter for wastewater is 280 mg/L [18]. The wastewater characteristics of Gümüşhane WWTP are as follows: BOD_5 = 280 mg/L, total nitrogen = 56 mg/L, total phosphorus (TP) = 10 mg/L and suspended solids (SS) = 291 mg/L. According to the wastewater characterization of Gümüşhane municipal wastewaters, the existing oxidation ditches and other units were built in 2011.

2.2. Numerical modeling and experimental study

Three models were studied for numerical analysis: Model 1, Model 2, and Model 3. Model 1 represents the Gümüşhane ODs with the current operating condition in which the experimental study was carried out. Model 2 is the Gümüşhane ODs with the project operation condition. And Model 3 is the new proposed model to improve the Gümüşhane ODs hydrodynamically.

2.2.1. Experimental study

The experimental study was carried out to validate the numerical analysis at the full-scale plant on-site measurements. The authors collected the velocity data from the full-scale Gümüşhane ODs. At the current operating conditions of the full-scale plant (2,443.33 m^3/d flow rate and V = 0.3466 m/s inlet velocities), measurements were picked at 14 points in ODs (Fig. 2). Measurements were performed at a depth of 0.85 m from the surface with the Acoustic Doppler Velocimeter (Nortek Vectrino Field Probe, P24213 Probe ID: VCN 8045) to minimize the effect of wind speed.

2.2.2. Numerical study

The CFD simulation of the 3 Models is given in forward in detail. Firstly, a CFD simulation of Model 1 was carried out to validate the experimental study. Secondly, the CFD simulation of Model 2 was carried out for detailed hydrodynamic analyses. And lastly, a numerical study of Model 3 was made for improving the Model 2.

In this study, the continuity and momentum equations of motion for a three-dimensional (3D) incompressible flow

Fig. 1. The Gümüşhane oxidation ditches.

Fig. 2. Pictures from Gümüşhane ODs field study.

were solved to calculate the single-phase flow of the ODs. In this study, the continuity and momentum equations of motion for a 3D incompressible flow were solved to calculate the single-phase flow of the ODs. For the fluid flow, based on the Reynolds-Averaged Navier-Stokes (RANS) equations, three-dimensional, steady, non-compressible flow is applied, and flow field calculations are made in a combined OD for the CFD analysis by ANSYS Fluent software (V13).

The conservation equations for mass and momentum are given in ANSYS Fluent and literature [19].

The standard k–ε model is a model depend on the model transport equations for turbulence kinetic energy (k) and turbulent dissipation rate (ε) and the renormalization group (RNG) k–ε model has a uniform form to the standard k–ε model [19].

Shih et al. [20] developed the realizable k–ε model to eliminate this lack of traditional k–ε models as follows:

- A new eddy-viscosity equation, including an inconstant $C\mu$ originally presented by Reynolds [21].

- A new model formula for dissipation (ε) based on the dynamic equation of the mean-square vorticity fluctuation.

In our study, although the water enters the ODs through pipes, there is channel flow in many parts of the ODs (Fig. 3). The ratio of the inertia force ρV^2L^2 to the viscous force is called the Reynolds number. Laminar flow changes transitional flow for most engineering applications at about Re ≤ 2,300, and turbulence flow begins at about Re ≥ 4,000 in straight pipes.

$$\mathrm{Re} = \frac{\text{inertia force}}{\text{viscous force}} = \frac{\rho VL}{\mu} = \frac{V \times D}{\nu} \tag{1}$$

where ρ is the density, V is the velocity, L is the characteristic length chosen as the diameter of the pipe (D), μ is the dynamic viscosity, ν is the kinematic viscosity.

For pipe flow, the flow is turbulent as determined by the Reynolds number below.

$$\mathrm{Re} = \frac{V \times D}{\nu}$$

$$\mathrm{Re} = \frac{0.3466\mathrm{m/s} \times 0.35\mathrm{m}}{1.003 \times 10^{-6}\,\mathrm{m^2/s}} = 120{,}947.16 > 4{,}000 \text{ turbulent} \tag{2}$$

For open-channel flow, the Reynolds number is generally defined as:

$$\mathrm{Re} = \frac{V \times R_h}{\nu} \tag{3}$$

where the hydraulic radius R_h is the characteristic length. Experiments have shown that laminar depends upon the cross-sectional geometry. Still, in many cases, it can be specified as Re < 500, and turbulence flow begins at bout Re > 1,000 in open channels.

$$V = \frac{Q}{A}$$

$$V = \frac{Q}{b \times h} \tag{4}$$

$$V = \frac{0.0283\mathrm{m^3/s}}{5\mathrm{m} \times 5.25\mathrm{m}} = 1.0781 \times 10^{-3}\,\mathrm{m/s}$$

$$\mathrm{Re} = \frac{V \times R_h}{v}$$

$$\text{The hydraulic radius is } R_h = A/P \rightarrow R_h = \frac{5\mathrm{m} \times 5.25\mathrm{m}}{5\mathrm{m} + 2 \times 5.25\mathrm{m}} = 1.69\mathrm{m}$$

$$\mathrm{Re} = \frac{1.0781 \times 10^{-3}\,\mathrm{m/s} \times 1.69\mathrm{m}}{1.003 \times 10^{-6}\,\mathrm{m^2/s}} = 1{,}816.54 > 1{,}000 \text{ turbulent} \tag{5}$$

2.2.3. Geometry and meshing

The geometry of the models are generated by Design Modeler and SpaceClaim in the ANSYS Workbench platform. According to the architectural project and data obtained from field observations, the geometry is designed on a full scale. Furthermore, the inlet and outlet, which are the pipe flow with an inner diameter of 35 and 50 cm for inlet and outlet, respectively, are also modeled.

Model 1 and Model 2 geometry for the Gümüşhane ODs model is the same. The designed geometry of the Gümüşhane ODs models with the dimensions and mesh structure is shown in Figs. 4 and 5. ODs heights are 6 m, the water layers at two ditches are 5.25 m, the lengths of ODs are 35 m, and the width of ODs is 10 m. Because of the design and construction errors, there are some differences between OD 1 and OD 2 geometries, such as guiding walls radius, extensions lengths, and position of the inlets, as shown in Fig. 4. The mesh is constructed with the tetrahedrons element structure, patch conforming method. Also, the body sizing method for ODs and edge sizing method for the pipe was applied to the geometry. After a series of grid-independent tests, which is given in Table 1, the total number of elements turned out to be 3 898 191. As seen in Fig. 5, the mesh density is increased, especially at the pipe-OD joints. The minimum and maximum element size are 5 and 20 cm, respectively.

Table 1
Grid-independent test

Element number	Outlet velocity, m/s
3898191	0.3703
5245608	0.3595
8575929	0.3888

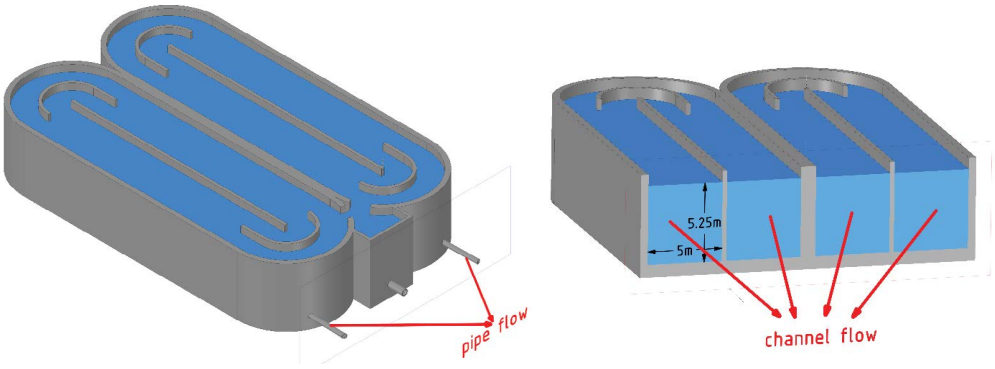

Fig. 3. The pipe and channel flow in the model.

Following the CFD analysis of the existing facility in the results and discussion section, the Model 2 geometry needs to improve hydrodynamically. Hence, a new original geometry named Model 3 was created to improve these hydrodynamically weak zones where the ditch flow decreased, dead zones were formed, and the current stopped. This geometry was created by struggling with many different designs. While creating the new geometry, the dimensions of the geometry were determined based on the volume of wastewater and the water retention time of the existing model. The aerators and mixers were not considered as mentioned before according to the aim of the study that determining the OD hydrodynamics except external momentum source. The main task of aerators and mixers is not to provide momentum for the flow. However, when they are operated in the pool, they have a positive effect on the flow. Here, suitable areas are left for their placement when necessary. The new model geometry and its dimensions are shown in Fig. 6.

The geometry parts created for a new model that differs from Model 2 geometry are given in Fig. 7. Looking at Fig. 7, the differences between the two geometries are shown below in items.

- *Change number 1*: While the height of the pool junction wall in the outlet section of Model 2 was 5.18 m, this wall was eliminated in Model 3.

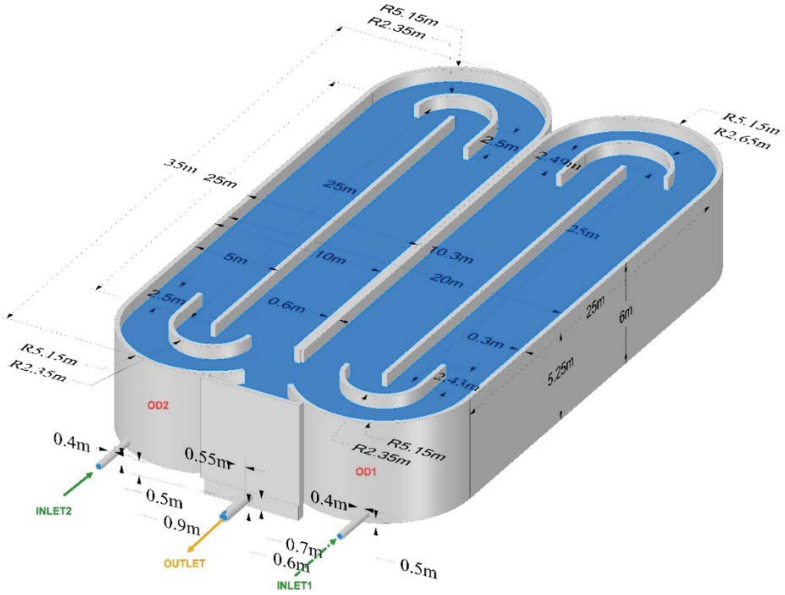

Fig. 4. The designed geometry of the Gümüşhane ODs model dimensions (Model 1 and Model 2).

Fig. 5. The designed model of Gümüşhane ODs mesh structure (Model 1 and Model 2).

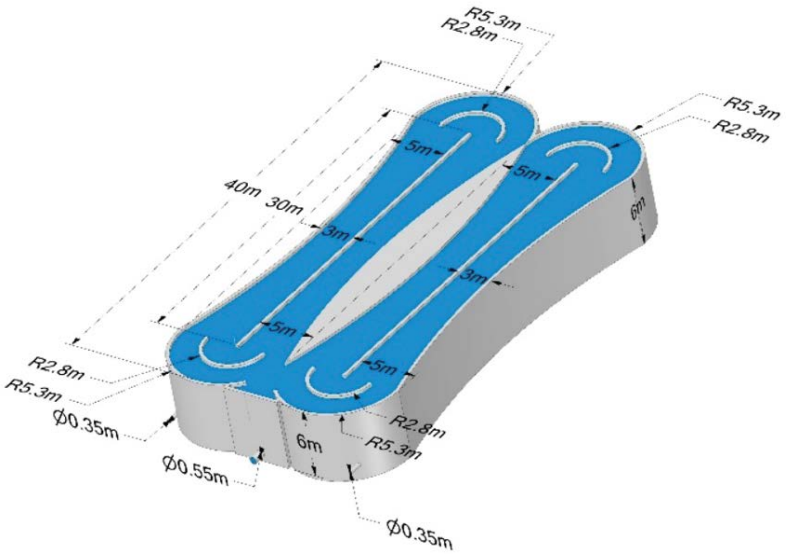

Fig. 6. The new model geometry and dimensions (Model 3).

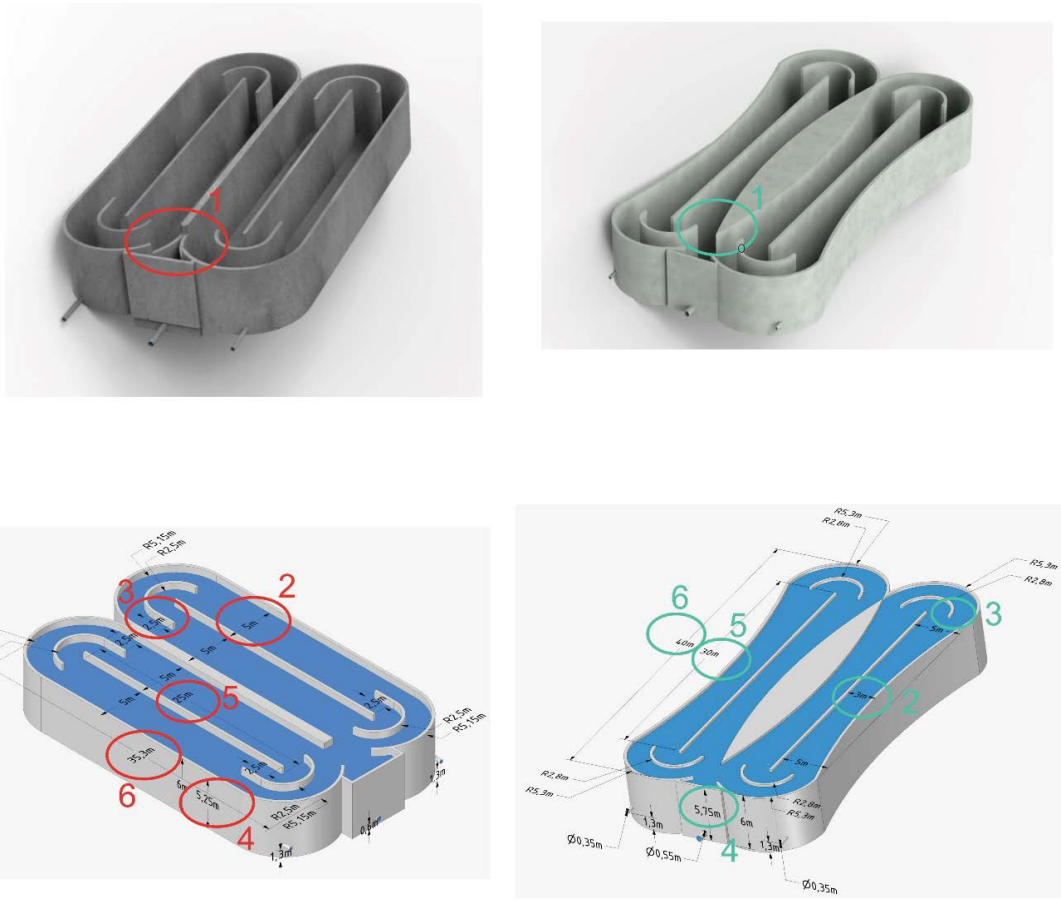

Fig. 7. Parts of Model 3 that differ from Model 2.

- *Change number 2*: The 5 m wide middle part of Model 2 has been reduced to 3 m in Model 3.
- *Change number 3*: 2.5 m extension of the small bend in Model 2 has been removed in Model 3
- *Change number 4*: The water height of 5.25 m in Model 2 has been increased to 5.75 m in Model 3.
- *Change number 5*: The length of the middle section, which was 25 m in Model 2, has been increased to 30 m in Model 3.
- *Change number 6*: The ditch length, 35.6 m in Model 2, has been increased to 40 m in Model 3.

The finite element network (mesh) was created by selecting the same settings in Model 2 with the 3,946,469 total number of elements, as shown in Fig. 8.

2.2.4. Boundary conditions

Simulation is performed in two cases for Gümüşhane ODs. One is currently operating conditions with 2,443.33 m^3/d flow rate and V = 0.3466 m/s inlet velocity for Model 1 to validate the simulated simulation model with field observations. Case 2 is the standard operating condition provided by the design project, which has the 8,312.65 m^3/d flow rate and V = 1 m/s inlet velocity for Model 2 and Model 3. The boundary conditions of the inlet and outlet are defined as "velocity-inlet" with the inflow velocity for the inlet 1 and inlet 2 and "pressure outlet". The top surface of the water layer is "symmetry", which is mean that "Symmetry plane imposes constraints that reflect the flow on both sides", and the solid boundaries were specified as "wall" and illustrated in Table 2 for three models (Fig. 9).

The criterion for convergence in the numerical model requires the scaled residuals to decrease to 10^{-6} for all equations.

The velocity inlet boundary value was 0.3466 m/s for Model 1, and three different turbulence models were implemented for a comparative study to verify the experimental study.

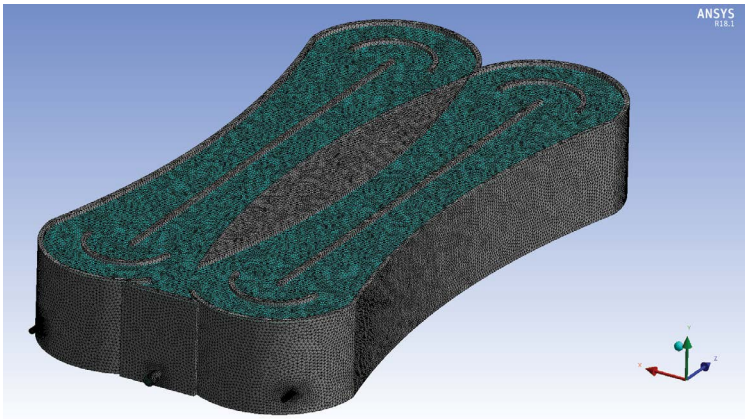

Fig. 8. Model 3 geometry mesh structure.

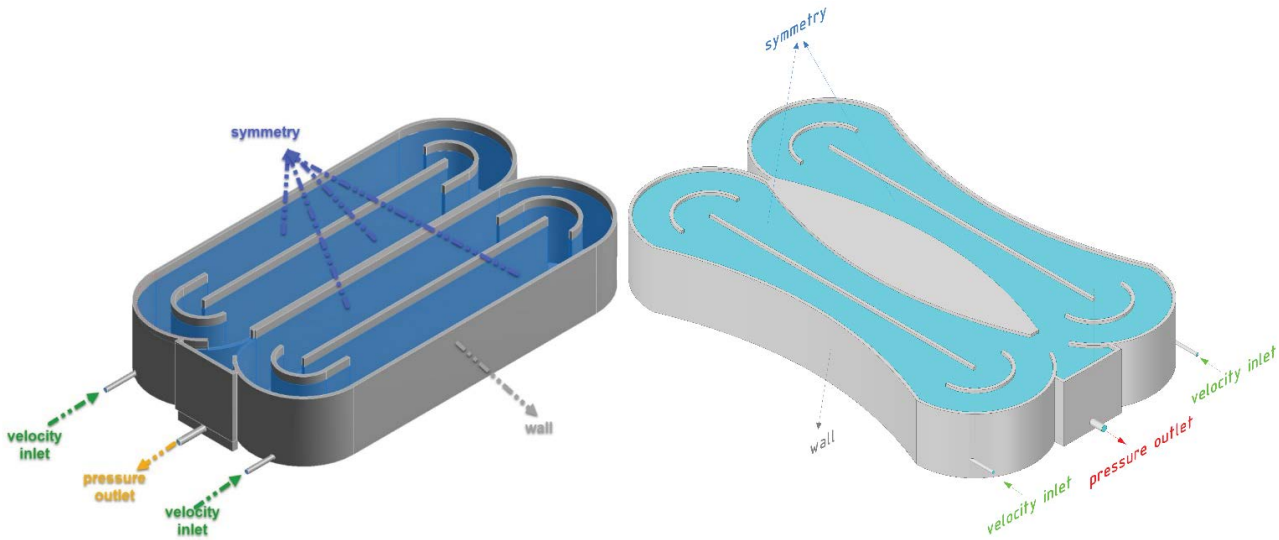

Fig. 9. The boundary conditions of the models.

Table 2
Boundary condition of models

Models	Boundary conditions				Turbulence models
	Velocity inlet	Outlet	Solids	Water surface	
Model 1	0.3466 m/s	Pressure outlet	Wall	Symmetry	ske, RNG, real
Model 2	1 m/s	Pressure outlet	Wall	Symmetry	ske
Model 3	1 m/s	Pressure outlet	Wall	Symmetry	ske

The CFD simulations of the Model 2 and Model 3 were carried out in a similar setup with Model 1. The only difference is the inlet velocity value of 1 m/s at the boundary conditions regarding the project design operation conditions and using the ske turbulence model, which gave the best predictive performance in validation.

The calculation time was approximately 48 h for the steady-state calculation on an Intel® Core™ computer with an i7-7500U CPU @ 2.70 GHz 2.90 GHz processor, 8.00 GB RAM, and a 64-bit operating system.

3. Results and discussion

Firstly, the field measurement result obtained from a full-scale plant is given in section 3.1. Secondly, the numerical study results of Model 1 for case 1 carried out to verify the experimental study are shown in the next section. Thirdly, the comparison of the numerical and experimental studies results is given in section 3.3. Fourthly, the results of the hydrodynamic analyses of Model 2 for case 2 carried out according to the turbulence model, which gave the best-predicted results are in Section 3.4. Lastly, the new proposed model numerical study results for Model 3 are provided in section 3.5.

3.1. Experimental data obtained full-scale plant measurement

Table 3 and Fig. 10 summarize the measurement results obtained from 14 points in the full-scale ODs. The velocities are varied from 0.820061 to 4.529205 cm/s. The maximum velocity was measured at location 14, whereas the minimum velocity was at location 10.

3.2. CFD simulation results of Model 1

Fig. 11 illustrates the distribution of velocity contours at a depth of 0.85 m from the surface in ODs based on the numerical results.

3.3. Comparison of the measurement data and simulation results for model verification

Fig. 12 shows the comparison of the field measurements with the simulation results.

It can be seen from Fig. 12 that field observations and simulation results were consistent with each other for ske, RNG, and real k–ε turbulence models with the relative error 13%, 17%, and 18%, respectively. Moreover, the most accurate prediction compared to the experimental findings belonged to the ske turbulence model. Generally, within 10%, lack of fit was considered a good simulation for CFD applications and within 20% considered acceptable [22]. In CFD analyses, errors below 10% may be deemed to be a good simulation, while errors below 20% may be considered acceptable [19].

3.4. CFD simulation results of Model 2

Firstly, the simulated velocity contours within a specific speed range (0–0.3 m/s) at a horizontal cross-section obtained from various depths in Model 2 are shown in Fig. 13.

The simulated velocity contours in Fig. 13 reveal that the water velocities increase from the surface towards the bottom. As is expected, the velocity is maximum at the inlet and outlet. This is because the wastewater enters from inlet 1 and inlet 2 with pipes with a diameter of 35.5 cm, whereby it acts as a water jet when it enters the ODs. The inlet velocity is 1 m/s, the outlet velocity is 1.20 m/s, and the mean velocity in Model 2 is 6.35×10^{-2} m/s. Fig. 13a shows the velocity fields, which vary between 0 and 0.48 m/s on the surface of the ODs. It can be seen from Fig. 13a that the velocity is higher in the linear extension of the outlet because the effluent of both OD emerges from a common point by narrowing the section. In Fig. 13b, considering the water height of 5.25 m in ODs, the velocity contour are shown along the length cross-section at the mid-point of the water-filled volume with y = 2.625 m. The velocity field is relatively homogenous, and the velocity value varies

Table 3
The average measurement velocities obtained from ODs

Location	Average measurement velocity, cm/s
1	2.978523
2	1.301461
3	1.554429
4	0.994786
5	0.947259
6	1.72618
7	2.613599
8	3.411818
9	1.734733
10	0.820061
11	1.750029
12	0.957079
13	3.097726
14	4.529205

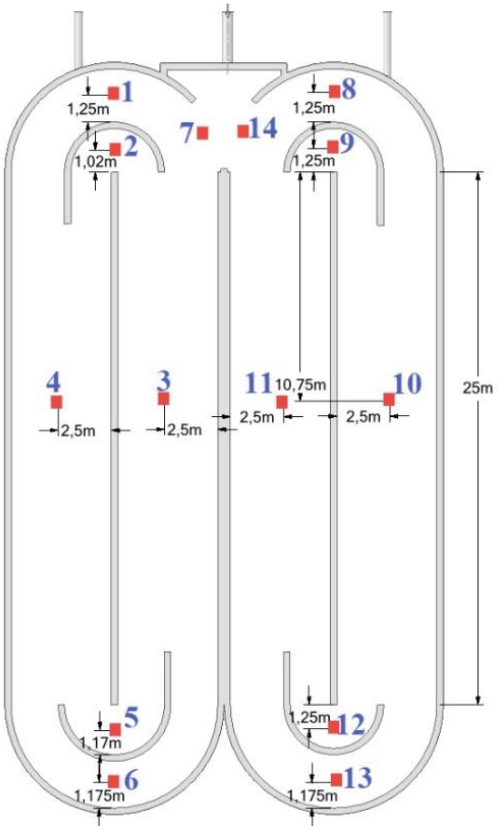

Fig. 10. Schematic view of measuring points in ODs.

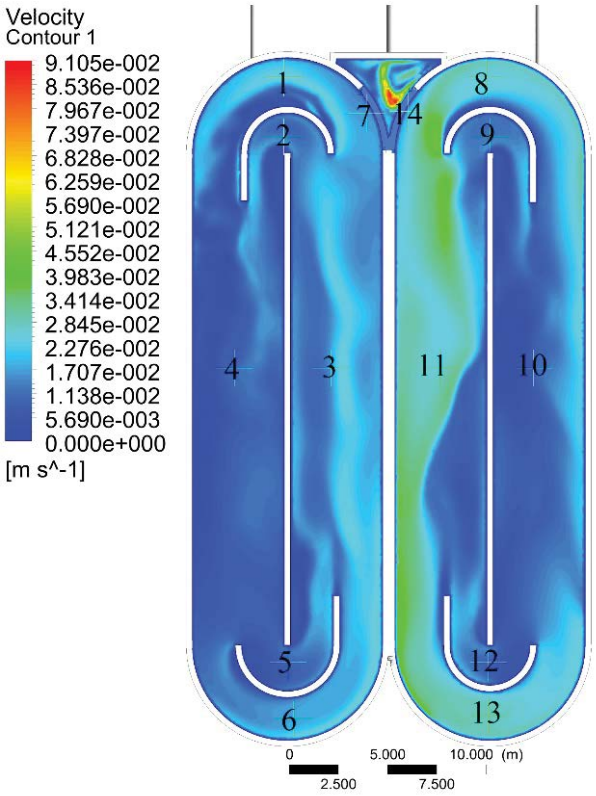

Fig. 11. Model 1 velocity contour distribution at a depth of 0.85 m from the surface.

from 0 to 0.13 m/s. When the simulated results at the inlet level in Fig. 13c are evaluated, the water jets, caused by pipe flow, do not proceed symmetrically at the two ODs due to the position of inlet 1, driven by design and construction error. The flow crashes to the guiding wall right in front of the inlet and is broken at OD 1; meanwhile, the flow continues without crashing and breaking along to the ditch at OD 2. In Fig. 13d, the bottom velocity field is shown, and, as it is seen, the velocity is maximum at the outlet (V = 1.20 m/s).

At the different vertical cross-sections, each 5 m, the simulated velocity contours are given in Fig. 14 within a specific speed range (0–0.3 m/s). The simulated results show that wastewater velocity is high in the linear extensions of the inlet and outlet. According to simulated results, because the wastewater velocity is high in the linear extensions of the inlet and outlet, as shown in Fig. 14, the inflow and outflow also play a significant role in the flow field except for the mechanical rotor and air diffusers.

Fig. 15 presents the simulated velocity streamlines in a specific speed range (0–0.3 m/s) and vectors in the global range. Fig. 15a and b show a notable difference between hydrodynamic behaviors of OD 1 and OD 2. Because inlet 1 and inlet 2 in the Gümüşhane ODs Model are non-symmetric, the velocity vectors and streamlines occur as illustrated in Fig. 15a and b, respectively. Moreover, Fig. 15a indicates that the number of streamlines and circulation rates in OD 2 is higher than in OD 1 due to the inlet 2. However, in OD 2, the wastewater generally travels around

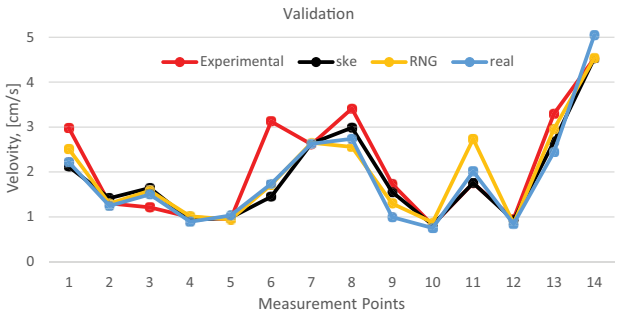

Fig. 12. Comparison of the measurement data with simulation results.

the edges of the walls and does not enter too much into the center partition. On the other hand, in OD 1, after the water enters from inlet 1, it crashes the small guide wall just in front of it and loses its initial speed and energy. Thus, the flow and cycle rate in the OD 1 are less than OD 2 and this causes the wastewater to accumulate and enter the middle partition in OD 1 more than OD 2.

According to simulated results, the wastewater velocity is high in the linear extensions of the inlets and outlet, as shown in Figs. 13–15. The velocity gradient is blue in other regions because the speeds are much lower than the inlet and outlet speeds.

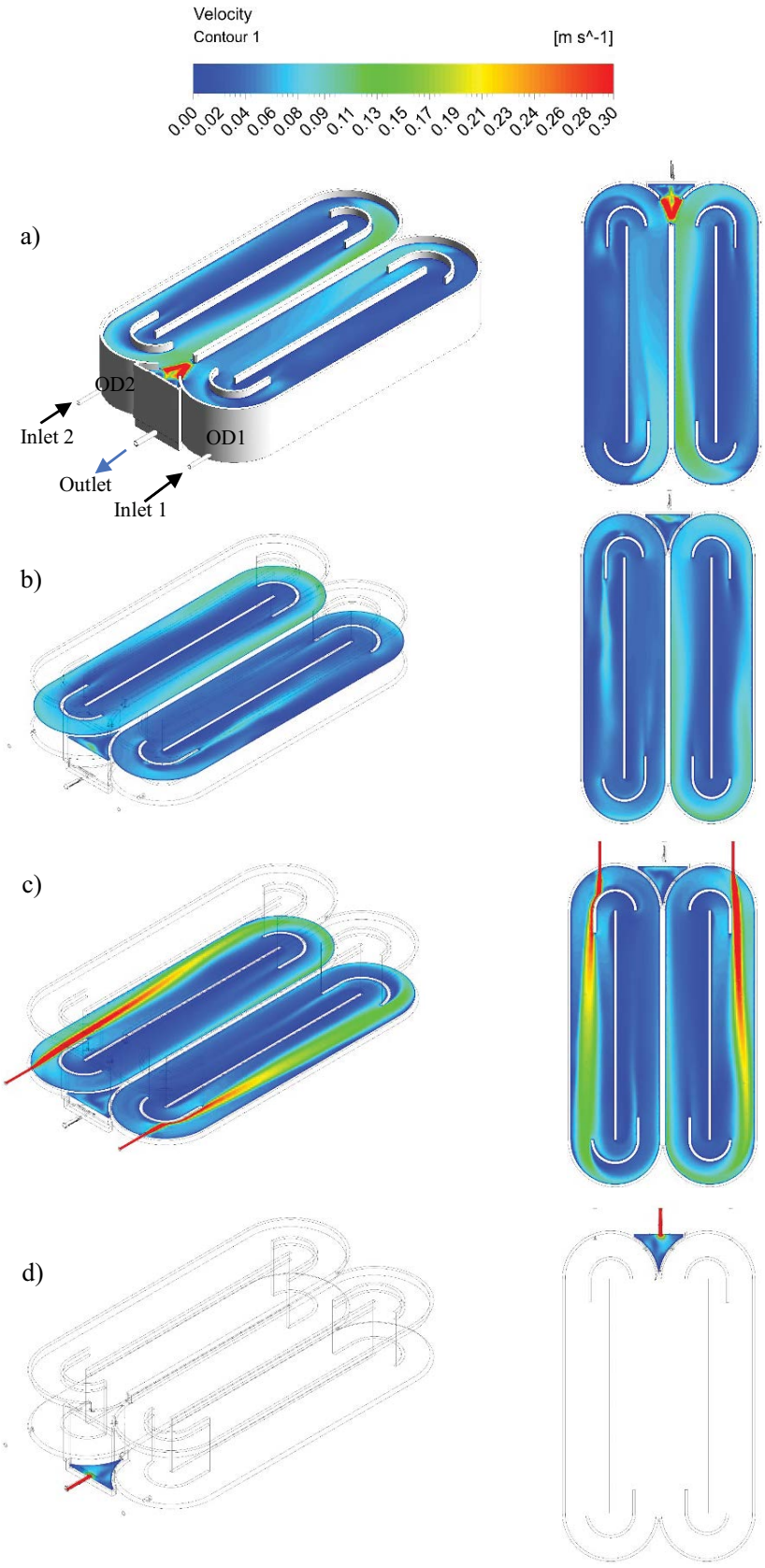

Fig. 13. The velocity contours of the Model 2 at various depths (a) the top surface of the water layer, y = 5.25 m, (b) middle of the water-layer, y = 2.625 m, (c) inlet level, y = 0.5 m and (d) outlet level, y = –0.5 m.

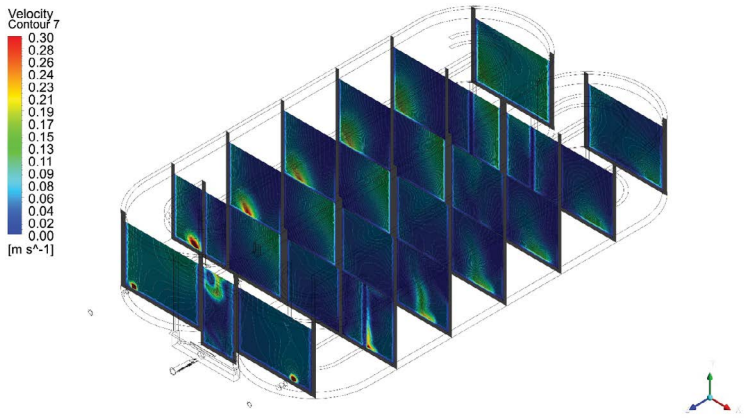

Fig. 14. The simulated velocity contours of the Gümüşhane ODs at a vertical cross-section every 5 m in ODs.

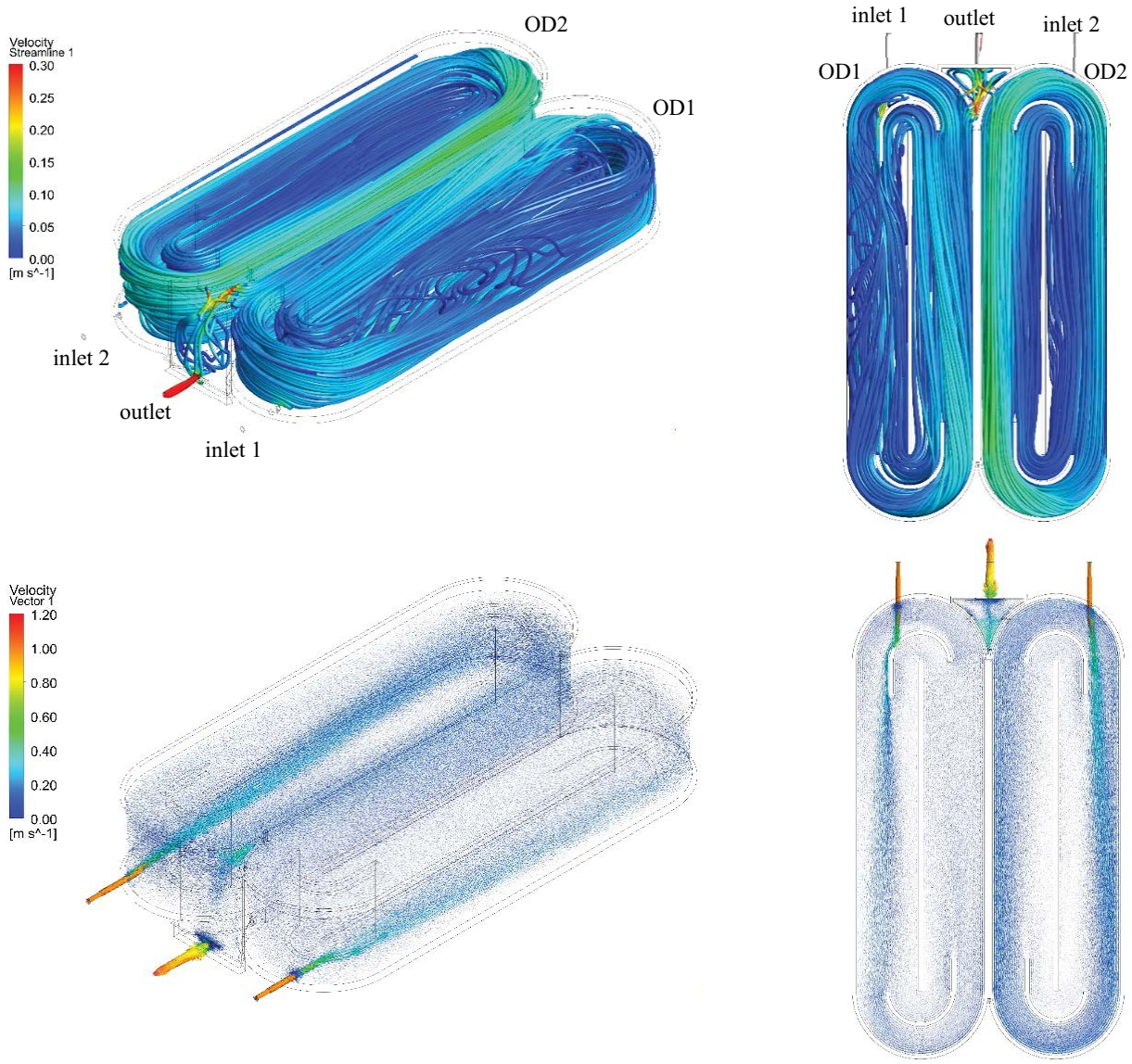

Fig. 15. The velocity streamlines and vectors in the Gümüşhane ODs model.

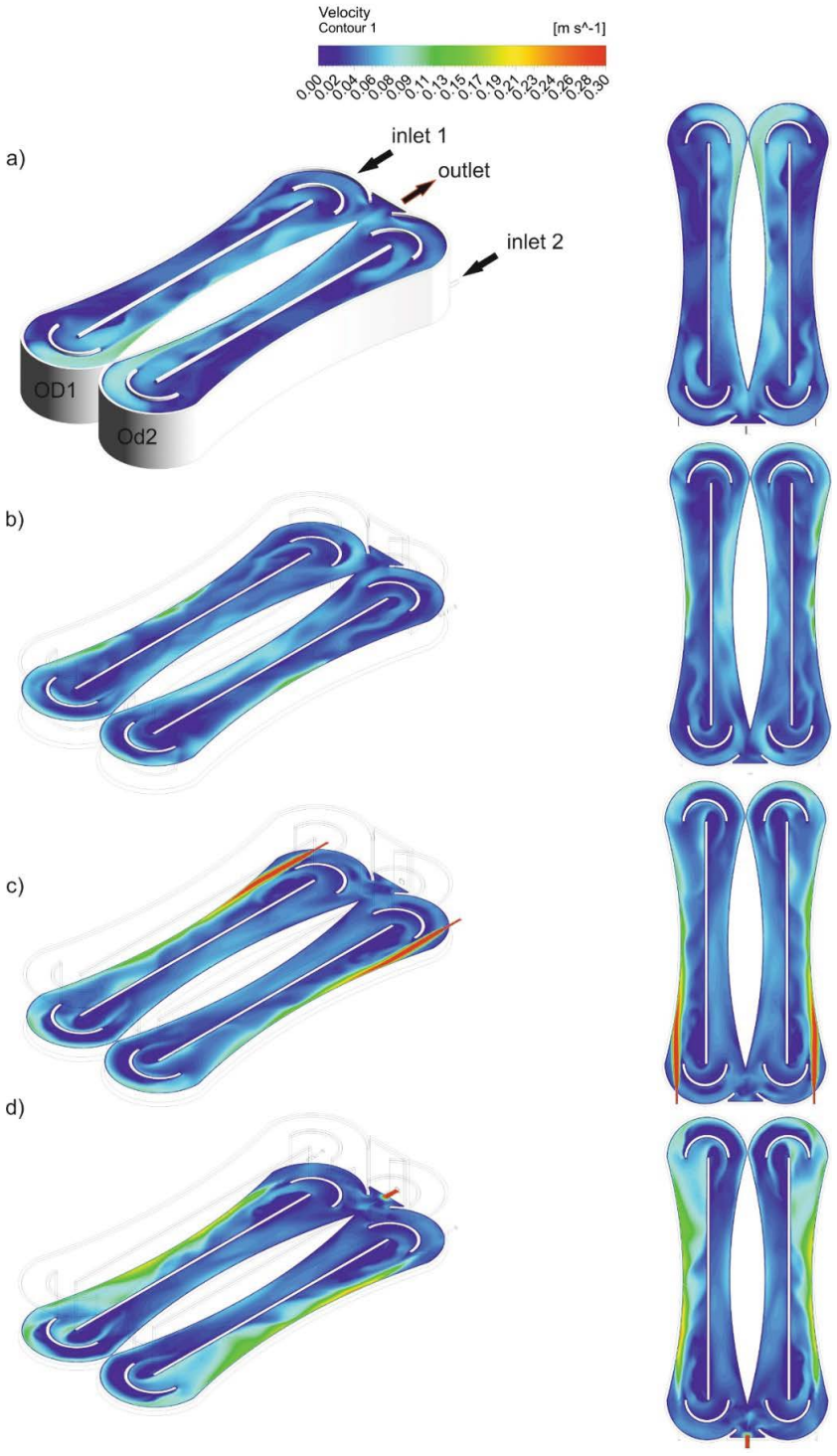

Fig. 16. The velocity contours of the Gümüşhane ODs at various depths (a) the top surface of the water layer, y = 5.75 m, (b) middle of the water-layer, y = 2.875 m, (c) inlet level, y = 1.3 m and (d) outlet level, y = –0.7 m.

These results show that the hydrodynamic characteristics of the simulated Gümüşhane ODs Models are inferior without external force such as air diffusers and rotors. The wastewater velocity should not exceed certain limits because of a biological WWTP (active sludge method-aeration pond-oxidation ditch). What is more, the minimum wastewater velocity should not drop below 0.2 m/s to avoid precipitation, and it is necessary to keep a sufficient amount of time (6–8 h) in OD. Thus the maximum wastewater velocity should be in the range of

0.8–1.5 m/s. However, the wastewater velocities are very low (≈0.06 m/s) in most areas of the Gümüşhane ODs, as can be seen from the simulated results above.

On the other hand, the inflow and outflow can be considered another energy source to drag the ditch flow except for mechanical rotors and aerators. Because the rotors and aerators are the key points of the biological treatment process of ODs, the traditional ODs are not conceived without rotors and aerators. They will be anyway in ODs design. But, this study aims not to ensure desired velocity values without rotors and aerators; it seeks to determine the hydrodynamic deficiencies of the existing geometry of ODs without any energy and momentum source and improve it. Thus, it helps to improve the operating conditions of ODs.

3.5. CFD simulation results of Model 3

As a result of 4,000 iterations, sufficient convergence was achieved, and the results were visualized. Primarily, velocity fields in ODs were found. The simulated velocity contours within a specific speed range (0–0.3 m/s) at a horizontal cross-section obtained from various depths in the new Model are shown in Fig. 16. The velocity fields of the top of the water level are given in Fig. 16a. Here, because the two ODs geometry is symmetrical, the velocity fields occur homogenously in the ditch, and the dead zones where the flow is stagnant are very few. Fig. 16b shows the velocity fields of the middle of the ODs. When the results are examined, it is seen that the green colors of legend dominate at this level. The velocity value is about 5,655 × 10^{-2} m/s, and there are relatively homogenously velocity fields in this water level. In the direction of the inlets, it is seen that the speeds are high at the edges of the ODs. Fig. 16c shows the velocity contours at the inlet level (y = 1.3 m). The water behaved like a water jet similar to Model 2 at the inlet level. It is a typical situation that the wastewater that comes out of a smaller pipe than the OD size at a certain velocity will show this effect. Again, similar to Model 2, the velocities in the direction of the inlets are significantly higher in ODs and gradually decrease as they move away from the inlets. Fig. 16d shows the velocity contours at outlet level that y = 0.7 m. As shown in Fig. 16d, the velocity is maximum at the outlet (V = 1.16 m/s).

The vertical fluid velocities obtained from various cross-sections with a limited velocity range (0–3 m/s) are shown in Fig. 17. When the figure is investigated, the inlet and outlet velocities are maximum, as is expected. In these points, because of the pipe flow, the water acts as a water jet and is dispersed in the ditches. Hence, the velocities in the ODs gradually decrease at the axis of the inlet and from this level to the top of the water. But the velocities relatively show homogenous distribution. The velocities don't vary much in the section of the two ODs join the outlet pipe since the water enters with the same flow rate from both ODs. The inlet velocity is 1 m/s, and the outlet velocity is 1.29 m/s. In other regions, the blue color is dominant in the velocity gradient, as the velocity is much smaller than the inlet and outlet velocities.

Fig. 18 presents the streamlines in ODs at a limited velocity range (0–0.3 m / sec). When these streamlines are examined, it is seen that the flow is homogeneously distributed in ODs. It is seen that the water cycle in ODs is also very homogeneous. Moreover, the vectorial representation of the distribution of inlet and outlet velocities in ODs and the trajectories of streamlines are presented in Fig. 18. As shown in the figure, there is a symmetrical velocity vector distribution in two ODs.

CFD results from Model 3 can be compared with the CFD results of Model 2, which shows the flow fields in ODs are more homogeneous than Model 2, as shown in Fig. 19. In general, when the velocities in the two models are compared, the average velocity, which is 6.63 cm/s in Model 2, is calculated as 4.95 cm/s in Model 3.

The organic matter found in wastewater is accomplished biologically using microorganisms used to oxidize the dissolved and particulate carbonaceous organic matter into simple end products. Most of these end products are formed as suspended solids either rise to the surface and accumulate in ODs, reducing the oxygen contact area of the organic content or, by the effect of gravity, they settle on the bottom of the ODs and block the mouth of the diffusers. These solid materials that settle and accumulate are undesirable in the biological treatment of wastewater.

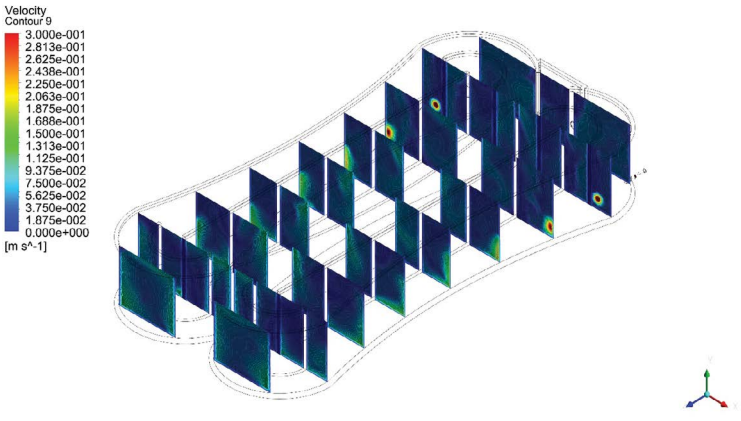

Fig. 17. The vertical fluid velocities obtained various cross-sections.

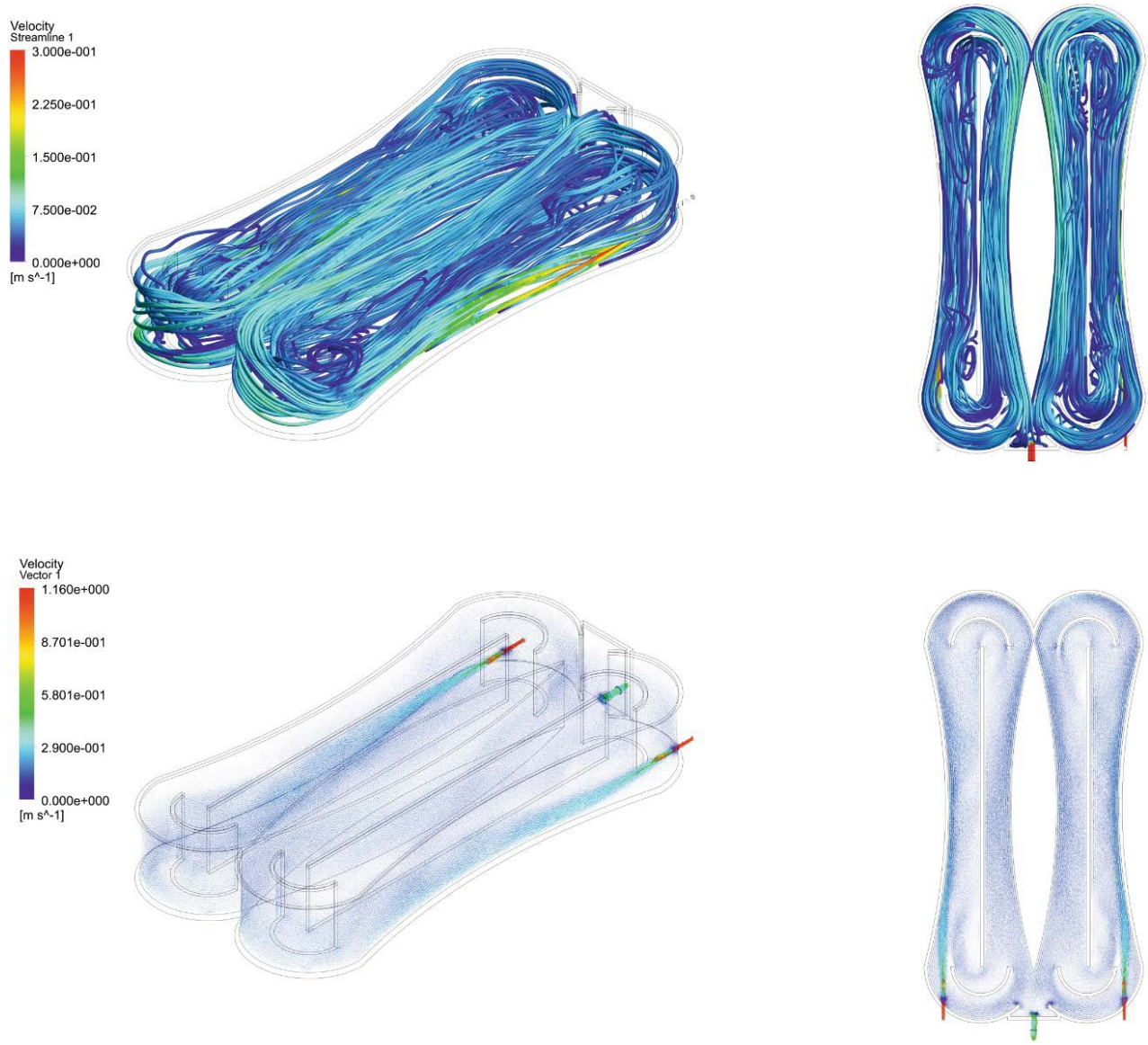

Fig. 18. The velocity streamlines and vectors of Model 3.

Therefore, it is essential to ensure a homogeneous flow and water cycle inside the ODs, to prevent these suspended solids from depositing to the bottom of accumulating on the surface. So, Model 3 is more successful than Model 2 when evaluated in this respect.

4. Conclusions

This study performed the hydrodynamic evaluation of the full-scale WWTPs with the experimentally validated numerical simulation using the CFD software ANSYS Fluent (V13). The results and suggestions obtained in this study are given below.

- The measurement results obtained in the actual plant were compared with the simulation results to validate the numerical model and achieve consistent results. Moreover, the measured and the simulated velocity data show the relative error of 13%, 17%, and 18% for ske, RNG, and real k–ε turbulence models, respectively.
- The most accurate prediction compared to the experimental findings belonged to the ske turbulence model.
- Hydrodynamic findings show that Model 2 is inferior without external forces such as air diffusers and rotors.
- The field measurement and numerical simulations reveal that there is no homogeneous flow field distribution in OD.
- The maximum wastewater velocity occurs at the inlet and outlet. The water velocity also decreases as it moves away from these points at vertical and horizontal.
- The inflow and outflow play a significant role in the flow field distribution in ODs. They can be considered another energy source to drag the ditch flow except for mechanical rotors and aerators. However, the

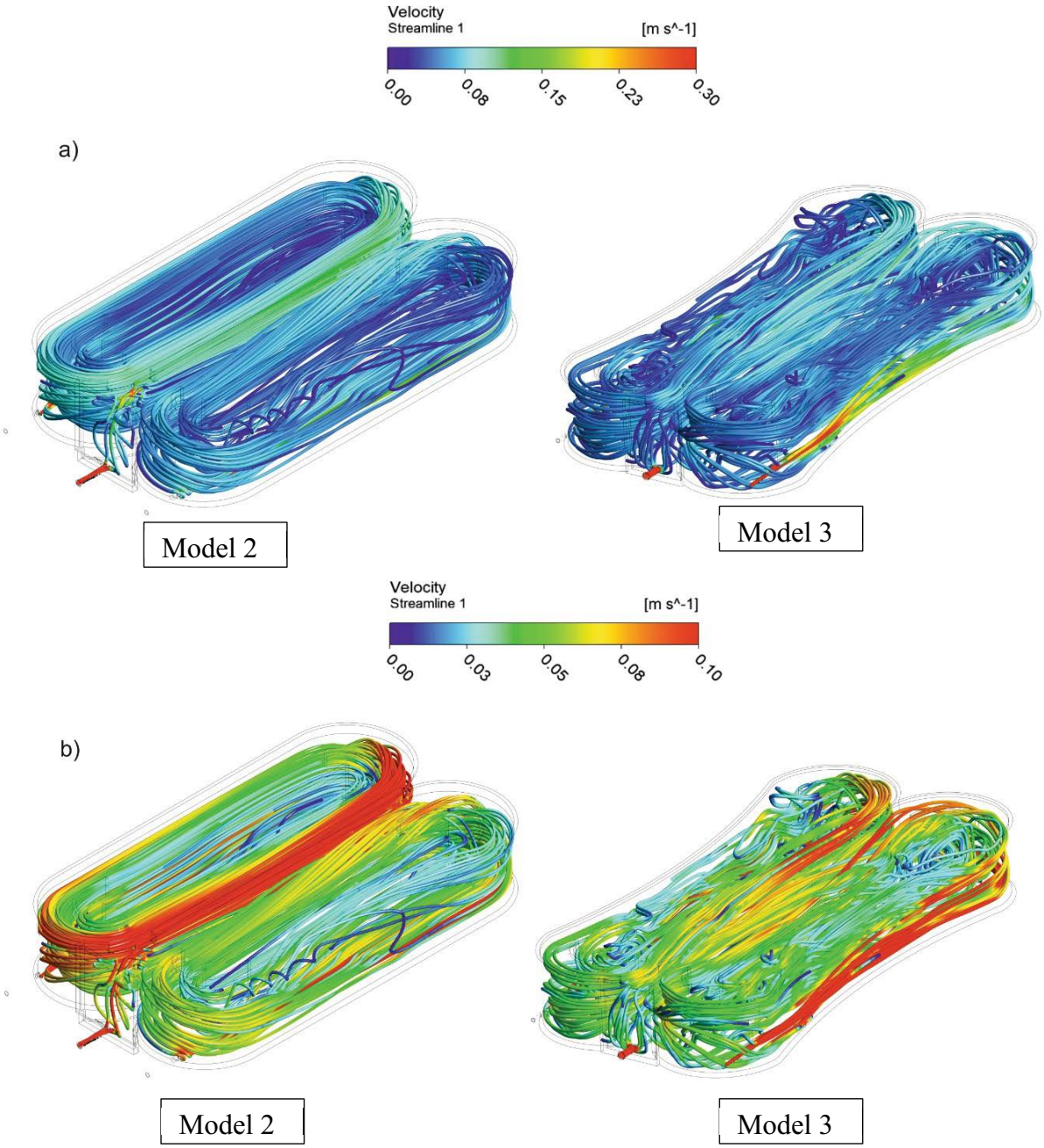

Fig. 19. The comparing of Model 2 and Model 3 via streamlines (a) velocity range of 0–0.3 m/s and (b) velocity range of 0–0.1 m/s.

findings of the current study do not support the previous research.

- The new proposed geometry (Model 3) was created to improve the hydrodynamical weakness of Gümüşhane ODs (Model 2) with homogenous flow fields, which is the primary concern of this facility in ODs. Hence, according to the continuity equation, the resultant velocities where the horizontal velocities are dominant have been increased and decreased by narrowing the sections, especially in the regions where the velocities are low and widening the sections in the regions where the velocities are high.
- Model 3 provides a more homogeneous flow field in ODs than Model 2. Therefore the operating costs caused by additional mechanical rotors and aerators to give a homogeneous flow field will be decreased. The present results are significant in at least two essential respects: treatment efficiency and energy consumption.

After this study, the following studies are recommended.

- A further study will be carried out to investigate different wall boundary conditions: Frictional, non-friction, sliding wall, non-slip wall, general wall equation, y^+ depth in the boundary layer between wall and liquid.

- Modeling of aerators in ODs and CFD analysis for two-phase flow (water-air): For the biological treatment of ODs, the oxygen provided by the aerators is in the gas phase, and the wastewater is in the liquid phase. Analysis of the dynamic effect of air diffusers in ODs as a source of momentum.
- Modeling of mixers in ODs and investigating the effect of mixers on flow characteristics in ODs by the mean of CFD: To model the results of the placement of mixers in different positions in the ODs on the flow fields as a source of momentum and the regional swirl and vortex motion that will be created to prevent the sedimentation of the solids in the ODs. Moreover, these analyzes will be carried out in three phases (solid–liquid–gas).
- And, finally, all these studies will be validated experimentally with new technological equipment such as high-frequency field Laser Doppler Velocimeter, Particle Doppler Anemometer.

Acknowledgments

I would like to thank Dr. Talia Ekin Tokyay for her help in improving my CFD knowledge. I would like to thank Dr. Enver Akaryalı, Dr. M. Ali Gücer, Dr. İbrahim Çavuşoğlu and Mr. Taner Demirel for helping the field observations. Also, I would like to thank Dr. Emre Özyurt for helping with this article's English grammar editing.

Symbols

A_a and A_s	—	Model constants
ADV	—	Acoustic Doppler Velocimeter
BOD	—	Biological oxygen demand
$C_{1\varepsilon}$	—	Constants
$C_{2\varepsilon}$	—	Constants
$C_{3\varepsilon}$	—	Constants
$C\mu$	—	Function of the mean strain and rotation rates
$\vec{F}$	—	External body forces
$F(M_t)$	—	Compressibility function
G_k	—	Formation of turbulence kinetic energy
G_b	—	Turbulence kinetic energy generated by buoyancy on calculated average velocity gradients
I	—	Unit tensor
K	—	Turbulence kinetic energy
p	—	Pressure
RANS	—	Reynolds-Averaged Navier-Stokes
RNG	—	Renormalization group model
real	—	Realizable k–ε model
S_m	—	Any mass and the user-defined source
ske	—	Standard k–ε model
t	—	Time
$\vec{v}$	—	Velocity vector
Y_M	—	Part of the undulating expansion in the compressible turbulence to the total distribution rate
ρ	—	Density
$\bar{\bar{\tau}}$	—	Stress tensor
μ	—	Molecular viscosity
σ_k and σ_ε	—	Turbulent Prandtl numbers for k and ε
ε	—	Turbulent dissipation rate
$\bar{\Omega}_{ij}$	—	Mean rate-of-rotation tensor

References

[1] M. Meister, D. Winkler, M. Rezavand, W. Rauch, Integrating hydrodynamics and biokinetics in wastewater treatment modelling by using smoothed particle hydrodynamics, Comput. Chem. Eng., 99 (2017) 1–12.
[2] A.M. Karpinska, J. Bridgeman, CFD-aided modelling of activated sludge systems – a critical review, Water Res., 88 (2016) 861–879.
[3] W. Chen, M. Xu, The two-dimensional simulation study of flow pattern near guiding wall of oxidation ditch, J. Water Resour. Prot., 2 (2010) 814–817.
[4] L. Fan, N. Xu, Z. Wang, H. Shi, PDA experiments and CFD simulation of a lab-scale oxidation ditch with surface aerators, Chem. Eng. Res. Des., 88 (2010) 23–33.
[5] W. Wei, Y. Liu, L. Bin, Numerical simulation of optimal submergence depth of impellers in an oxidation ditch, Desal. Water Treat., 57 (2016) 8228–8235.
[6] Y. Zhang, Y. Zheng, E. Fernandez-Rodriguez, C. Yang, Y. Zhu, H. Liu, H. Jiang, Optimization design of submerged propeller in oxidation ditch by computational fluid dynamics and comparison with experiments, Water Sci. Technol., 74 (2016) 681–690.
[7] J. Climent, R. Martínez-Cuenca, P. Carratalà, M.J. González-Ortega, M. Abellán, G. Monrós, S. Chiva, A comprehensive hydrodynamic analysis of a full-scale oxidation ditch using Population Balance Modelling in CFD simulation, Chem. Eng. J., 374 (2019) 760–775.
[8] Y. Yang, Y. Wu, X. Yang, K. Zhang, J. Yang, Flow field prediction in full-scale carrousel oxidation ditch by using computational fluid dynamics, Water Sci. Technol., 62 (2010) 256–265.
[9] Y. Yang, J. Yang, J. Zuo, Y. Li, S. He, X. Yang, K. Zhang, Study on two operating conditions of a full-scale oxidation ditch for optimization of energy consumption and effluent quality by using CFD model, Water Res., 45 (2011) 3439–3452.
[10] W. Huang, K. Li, G. Wang, Y. Wang, Computational fluid dynamics simulation of flows in an oxidation ditch driven by a new surface aerator, Environ. Eng. Sci., 30 (2013) 663–671.
[11] L. Lei, J. Ni, Three-dimensional three-phase model for simulation of hydrodynamics, oxygen mass transfer, carbon oxidation, nitrification and denitrification in an oxidation ditch, Water Res., 53 (2014) 200–214.
[12] H. Xie, J. Yang, Y. Hu, H. Zhang, Y. Yang, K. Zhang, X. Zhu, Y. Li, C. Yang, Simulation of flow field and sludge settling in a full-scale oxidation ditch by using a two-phase flow CFD model, Chem. Eng. Sci., 109 (2014) 296–305.
[13] A.M. Karpinska, M.M. Dias, R.A.R. Boaventura, R.J. Santos, Modeling of the hydrodynamics and energy expenditure of oxidation ditch aerated with hydrojets using CFD codes, Water Qual. Res. J. Can., 50 (2015) 83–94.
[14] W. Wei, Z. Zhang, Y. Zheng, Y. Liu, Numerical simulation of additional guiding baffles to improve velocity distribution in an oxidation ditch, Desal. Water Treat., 57 (2016) 24257–24266.
[15] W. Wei, Y. Bai, Y. Liu, Optimization of submerged depth of surface aerators for a carrousel oxidation ditch based on large eddy simulation with Smagorinsky model, Water Sci. Technol., 73 (2016) 1608–1618.
[16] A.I. Stamou, Prediction of Hydrodynamic Characteristic of Oxidation Ditches Using the k–ε Turbulence Model, 2nd Int. Symp. Eng. Turbul. Model. Meas., Florance, Italy, 1993, pp. 261–271.
[17] L. Luo, W. Li, Y. Deng, T. Wang, Numerical simulation of a combined oxidation ditch flow using 3D k–ε turbulence model, J. Environ. Sci., 17 (2005) 808–812.
[18] R. Sibil, M. Berkun, S. Bekiroglu, The comparison of different mathematical methods to determine the BOD parameters,

a new developed method and impacts of these parameters variations on the design of WWTPs, Appl. Math. Modell., 38 (2014) 641–658.
[19] ANSYS Fluent, ANSYS Fluent, 2013.
[20] T.H. Shih, W.W. Liou, A. Shabbir, Z. Yang, J. Zhu, A new k–ε eddy viscosity model for high Reynolds number turbulent flows, Comput. Fluids, 24 (1995) 227–238.
[21] W.C. Reynolds, Fundamentals of Turbulence for Turbulence Modelling and Simulation, Lecture Notes von Karman Insitute, 1987, pp. 1–66.
[22] H.X. Littleton, G.T. Daigger, P.F. Strom, Application of computational fluid dynamics to closed-loop bioreactors: I. characterization and simulation of fluid-flow pattern and oxygen transfer, Water Environ. Res., 79 (2007) 600–612.